Biointerphases
A Journal of Biomaterials and Biological Interfaces

UV- and thermally-active small bi-functional gelator for creating gradient polymer network coatings

Cite as: Biointerphases **18**, 011001 (2023); https://doi.org/10.1116/6.0002268
Submitted: 09 October 2022 • Accepted: 14 December 2022 • Published Online: 10 January 2023

Pandiyarajan Chinnayan Kannan and Jan Genzer

COLLECTIONS

Paper published as part of the special topic on Special Topic Collection: Polymeric Biointerfaces A Collection in celebration of Nicholas D. Spencers career

Biointerphases
A Journal of Biomaterials and Biological Interfaces

ARTICLE

avs.scitation.org/journal/bip

UV- and thermally-active small bi-functional gelator for creating gradient polymer network coatings

Cite as: Biointerphases 18, 011001 (2023); doi: 10.1116/6.0002268
Submitted: 9 October 2022 · Accepted: 14 December 2022 ·
Published Online: 10 January 2023

Pandiyarajan Chinnayan Kannan[1,a] and Jan Genzer[1,2,b]

AFFILIATIONS

[1]Department of Chemical and Biomolecular Engineering, North Carolina State University, Raleigh, North Carolina 27695-7905
[2]Global Station for Soft Matter, Global Institution for Collaborative Research and Education (GI-CoRE), Hokkaido University, Hokkaido 060-0808, Japan

Note: This paper is part of the Biointerphases Special Topic Collection on Polymeric Biointerfaces A collection in celebration of Nicholas D. Spencer's career.

[a]**Current address:** Corning Inc., Painted Post, New York 14870.
[b]**Author to whom correspondence should be addressed:** jgenzer@ncsu.edu

ABSTRACT

We present a versatile one-pot synthesis method for creating surface-anchored orthogonal gradient networks using a small bi-functional gelator, 4-azidosulfonylphenethyltrimethoxysilane (4-ASPTMS). The sulfonyl azide (SAz) group of 4-ASPTMS is UV (≤254 nm) and thermally active (≥100 °C) and, thus, enables us to vary the cross-link density in orthogonal directions by controlling the activation of SAz groups via UV and temperature means. We deposit a thin layer (∼200 nm) of a mixture comprising ∼90% precursor polymer and ∼10% 4-ASPTMS in a silicon wafer. Upon UV irradiation or annealing the layers, SAz releases nitrogen by forming singlet and triplet nitrenes that concurrently react with any C–H bond in the vicinity leading to sulfonamide cross-links. Condensation among trimethoxy groups in the bulk connects 4-ASPTMS units and completes the cross-linking. Simultaneously, 4-ASPTMS near the substrate reacts with surface-bound –OH motifs that anchor the cross-linked polymer chains to the substrate. We demonstrate the generation of orthogonal gradient network coatings exhibiting cross-link density (or stiffness) gradients in orthogonal directions using such a simple process.

I. INTRODUCTION

The research on gradient materials is evolving due to their potential biological applications[1] and materials discovery.[2] Gradient materials exhibit a continuous variation in any physical or chemical properties, e.g., stiffness or wettability.[2] Achilles tendon is an excellent example of stiffness gradients that connect soft muscle tissues and hard bones.[3] Mimicking such gradients using synthetic materials will tremendously impact artificial implants and tissue engineering.[4] Several efforts aim at synthesizing polymeric gradient materials[3] and surface-bound gradients.[5] Some advancements include creating surface-anchored polymer brushes presenting gradients in grafting density[6] and molecular weight.[2] However, polymer brush-based gradient applications are constrained due to their sophisticated synthetic protocols (using transition metals and ligands), limited thickness, and stability.[7,8]

In the past, we generated surface-anchored gradient networks by synthesizing a copolymer comprising 90 mol. % of *N*-isopropyl acrylamide, 5 mole % of UV-active methacryloyloxy benzophenone (MABP),[9] and 5 mol. % of thermally active styrene sulfonyl azide (SSAz).[10] The gel stiffness was regulated spatially by adjusting the UV dose and temperature independently in opposite directions, resulting in orthogonal gradient networks displaying gradients in cross-link density or stiffness. However, this method involves a complex multistep synthesis of MABP, SSAz, and surface anchors (e.g., silane-bearing benzophenone or sulfonyl azide functionalities), limiting its applications. Therefore, developing versatile and cost-effective techniques employing inexpensive common polymers is inevitable for many industrial applications.

Herein, we report a robust one-step synthesis technique for creating gradient network coatings employing a small bi-functional

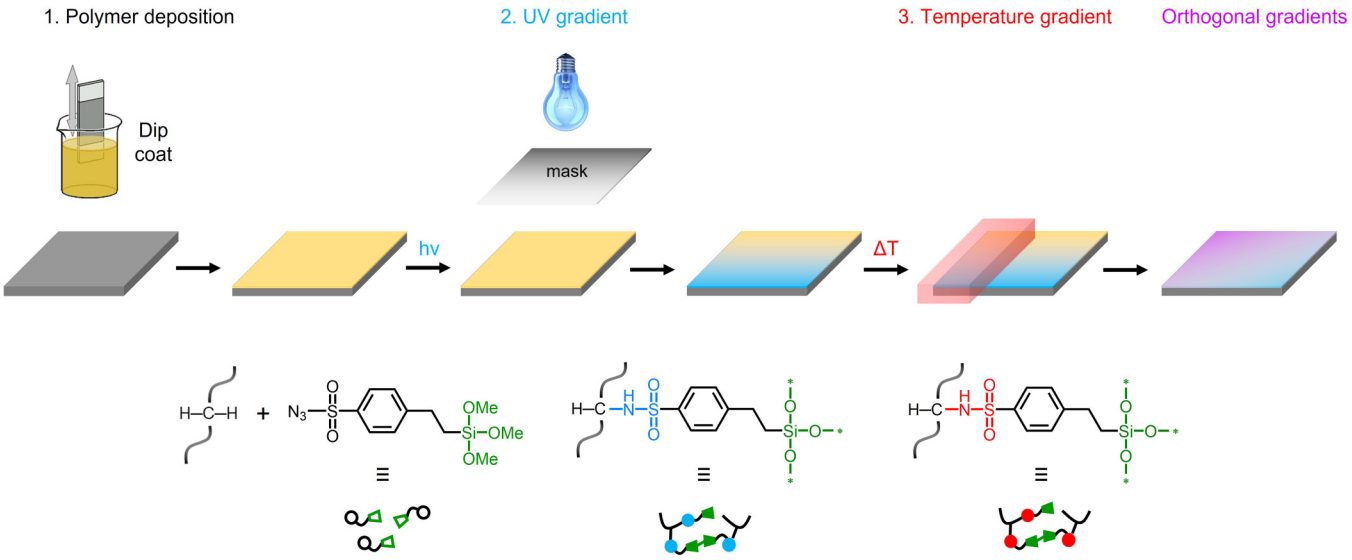

FIG. 1. Schematics of UV/thermal orthogonal gradient networks where the PVP/4-azidosulfonylphenethyltrimethoxysilane (4-ASPTMS) film was deposited on a silicon wafer. A photomask was used to adjust the UV dose, or the sample was moved under the UV light to produce gradients in UV-activated cross-links. The sample was then placed on top of a hot gradient stage (orthogonally to the UV cross-linking direction) to achieve a gradient in thermally activated cross-links. Subsequently, the sample was extracted with methanol to remove any unreacted polymeric material or macromolecules that are not part of the network coatings.

gelator, 4-azidosulfonyl phenethyl trimethoxysilane (4-ASPTMS). We deposited a thin layer (~200 nm) of PVP/10% 4-ASPTMS mixture on a silicon wafer and cross-linked by UV irradiation and heating the layers. 4-ASPTMS enables simultaneous cross-linking and surface-attachment reactions. We adjust the degree of cross-linking or gel density by controlling the UV dose and temperature in a gradient fashion. We systematically investigate the gel formation using spectroscopic ellipsometry (SE) and Fourier-transform infrared spectroscopy in the attenuated total reflection mode (FTIR-ATR). The results demonstrate that 4-ASPTMS is efficient in spatially varying the matrix's gel fraction (cross-link density or stiffness) in orthogonal directions by adjusting the UV dose and temperature (cf. Fig. 1). Our user-friendly technique works for any polymer or substrate as long as it contains C–H or –OH bonds.

II. EXPERIMENT

A. Materials

Polyvinylpyrrolidone (PVP) (molecular weight, 360 kDa) was purchased from Sigma-Aldrich (St. Louis, MO, USA) and used without further purification. 4-ASPTMS was acquired from Gelest (Morrisville, PA, USA). Methanol was purchased from Fisher Scientific (Pittsburgh, PA, USA). Silicon wafers were purchased from Silicon Valley Microelectronics (Santa Clara, CA, USA) (orientation, [100]; thickness, 0.5 mm; and diameter, 100 mm).

B. Instrumentation

Variable angle spectroscopic ellipsometry (VASE, J.A. Woollam, USA) was used to measure film thicknesses. Thermal cross-linking was produced using an FP82HT Hot stage with an FP90 Central Processor (Mettler Toledo, USA). A custom designed hot gradient stage was employed for producing thermal gradient samples. Photo cross-linking reactions were performed using an OmniCure series-1000 UV lamp (Lumen Dynamics, Canada). UV light intensity was measured using an ILT-1400-A radiometer-photometer (International Light Technology, USA). In all experiments, the UV lamp was warmed for 5–10 min before the cross-linking reactions for reproducibility. A dip coater (KSV-NIMA, USA) was used to move the sample under the UV light for making photo gradient surfaces. The polymer film was deposited using a spin coater (PNM32 model, Headway Research, Inc., USA).

C. Preparation of surface-anchored networks

A solution containing a calculated amount of polymer (e.g., 360 mg; i.e., 90% weight fraction) and 4-ASPTMS (40 mg; i.e., 10% weight fraction) was prepared with a total concentration of 20 mg/ml, i.e., 400 mg in 20 ml of methanol. The polymer solution was deposited onto a clean silicon wafer using a dip-coating (KSV NIMA Single Vessel Dip Coater) technique at 100 mm/min. The film was annealed at 60–70 °C (no cross-linking occurs) for 10 min to remove the solvent and irradiated with UV light (254 nm, UV incident power = 50 mW/cm^2) or annealed (at 140 °C) that led to simultaneous cross-linking and the surface attachment of polymer coatings. Subsequently, the layers were extracted in methanol overnight to remove any unreacted or loosely bound materials from the surface. The film was dried with nitrogen air and annealed at an elevated temperature (60–70 °C) to remove the solvent. Then, the layer thickness was measured using SE.

D. Preparation of gradient network films

As described above, a precursor polymer film was deposited on a silicon wafer with a specific dimension (e.g., $5 \times 5\ cm^2$). The sample was placed on a gradient heating stage for thermal gradient networks and cross-linked for 2.5 h twice. This process creates a temperature gradient ranging from 140 to 65 °C. The horizontal gradients in temperature were obtained by heating the sample at one end, and the other end of the sample rested at room temperature. For the photo gradient networks, the specimen was either moved under UV light with a rate of 1 cm/min for 5 min or used as a photomask to adjust the UV dose. After photo- or thermal cross-linking, the sample was extracted with methanol (overnight) to remove any unreacted polymer or macromolecules from the substrate surface. The film thickness of the deposited layer was measured using SE.

E. Polymer characterization

Fourier-transform infrared spectroscopy was used to characterize the polymer films in the attenuated total reflection mode (FTIR-ATR) (Nicolet 6700 Spectrometer, Thermo Electron, USA). 128 scans were collected for each sample studied after recording the background signal using a DTGS TEC detector with a scan resolution of 4 cm^{-1} between 600 and 4000 cm^{-1}.

F. Gel fraction using spectroscopic ellipsometry

The gel fraction was calculated from the change in the film thickness before (d_0) and after (d) extraction of the cross-linked polymer as described in Eq. (1). The film thickness was measured using variable angle spectroscopic ellipsometry. Reflectivity scans were collected at a 70° angle of incidence (relative to the vertical direction) in the spectral range of ($\lambda = \alpha$) 400−1000 nm in 60 steps (10 nm/step). Measurements were made on the UVO-cleaned silicon wafer deposited with the polymer. The ellipsometry data were modeled using the Fresnel formalism comprising a three-layer model in WVASE32 software (J.A. Woollam Co., version 3.682): Layer 1: Si substrate, layer 2: SiO_2 (1.5–1.7 nm thick), and layer 3: polymer ad-layer (the refractive index was modeled as a Cauchy function, $n = A_n + \frac{B_n}{\lambda^2}$; $A_n = 1.48–1.5$ and $B_n = 0.01\,\mu m^2$ are the fitting parameters).

III. RESULTS AND DISCUSSION

In making gradient network coatings (cf. Fig. 1), it is quintessential to identify and optimize the cross-linking condition, which leads to gel formation. First, we explored the thermal cross-linking of 4-ASPTMS by depositing a thin layer (~200 nm) of the PVP (90%) and 4-ASPTMS (10%) mixture on a silicon wafer and annealed at different temperatures (70–140 °C) and times (0–600 min). Any unreacted or loosely bound materials or macromolecules that are not part of the network are removed by extracting the layers in methanol overnight. Next, we determined the gel fraction (P_{gel}) of cross-linked networks from the ratio of the film thickness before (d_0) and after extraction (d) and plotted against the annealing temperature [cf. Fig. 2(a)] and time [cf. Fig. 2(b)],

$$P_{gel} = \frac{d}{d_0}, \tag{1}$$

where d is the film thickness after extraction and d_0 is the film thickness before extraction. The sulfonyl azide (SAz) cross-linking mechanism has recently been reported in our previous publications.[10,11] Briefly, upon heating the PVP/10% 4-ASPTMS layer, the SAz groups release nitrogen gas and form singlet and triplet nitrenes. The resultant nitrenes undergo a C–H insertion cross-linking (CHiC) reaction with neighboring polymer chains that form sulfonamide cross-links.[12,13] The trimethoxysilane groups in 4-ASPTMS undergo self-condensation and create siloxane linkages that complete the cross-linking process. Concurrently, 4-ASPTMS molecules present near the substrate react with surface hydroxyl groups that facilitate the attachment of cross-linked network.[11] Such a simple process allows simultaneous network formation and the surface attachment of the cross-linked polymer layers.

The silicon wafer ($1 \times 5\ cm^2$) was dip-coated with a PVP/10% 4-ASPTMS layer and placed on a hot stage where the temperature varied from 70 to 140 °C in a gradient fashion. The sample was annealed for 300 min, and the temperature at different locations was recorded using several thermocouples placed at various positions along the heat stage. The sample displayed a continuous color variation depending on annealing temperature, implying a change in the film thickness from which P_{gel} is determined [cf. Fig. 2(a)]. It resulted in uni-directional gradient network layers displaying progressive variations in P_{gel}. A key advantage of employing gradient samples is that a single specimen can investigate a range of temperatures and their influence on gelation that requires several individual specimens. The regions annealed below 90 °C showed no gel formation, i.e., $P_{gel} \leq 0.02$. In contrast, the areas in the sample annealed at above 100 °C displayed gelation, and the maximum gel fraction was attained at 140 °C ($P_{gel} = 0.80$). The results are consistent with our previous attempt on PVP/6-ASHTES (6-azidosulfonyl hexyl triethoxysilane), where annealing layers at 140 °C for 300 min produced the maximum gel fraction.[11]

After establishing the annealing temperature (140 °C), we studied the gel kinetics of PVP/10% 4-ASPTMS layers by plotting P_{gel} against the annealing time [cf. Fig. 2(b)]. P_{gel} increased with time and reached maximum gelation after 300 min ($P_{gel} \sim 0.80$). The inset in Fig. 2(b) shows the FTIR-ATR spectra of films annealed for various times (0–300 min). A progressive attenuation in the absorbance of the azide functionality ($N = N^+ = N^-$) at 2130 cm^{-1} reveals that the azide groups are consumed gradually during the reaction. A near disappearance of the azide peak after 300 min suggests that almost all azide groups have been converted into sulfonamide links. This result agrees with the gel kinetics data obtained from film thickness measurements, which show a maximum $P_{gel} \sim 0.80$ after 300 min of annealing. These experiments allowed us to optimize the thermal reaction conditions, i.e., annealing temperature and time for creating surface-anchored network coatings.

To investigate the UV-cross-linking reaction of 4-ASPTMS, we deposited a thin layer (~200 nm) of PVP/10% 4-ASPTMS mixture on a silicon wafer ($1 \times 5\ cm^2$). After evaporating the solvent, the layers were exposed to UV light at 254 nm (UV incident power = 50 mW/cm^2) at various times. We adjusted the UV

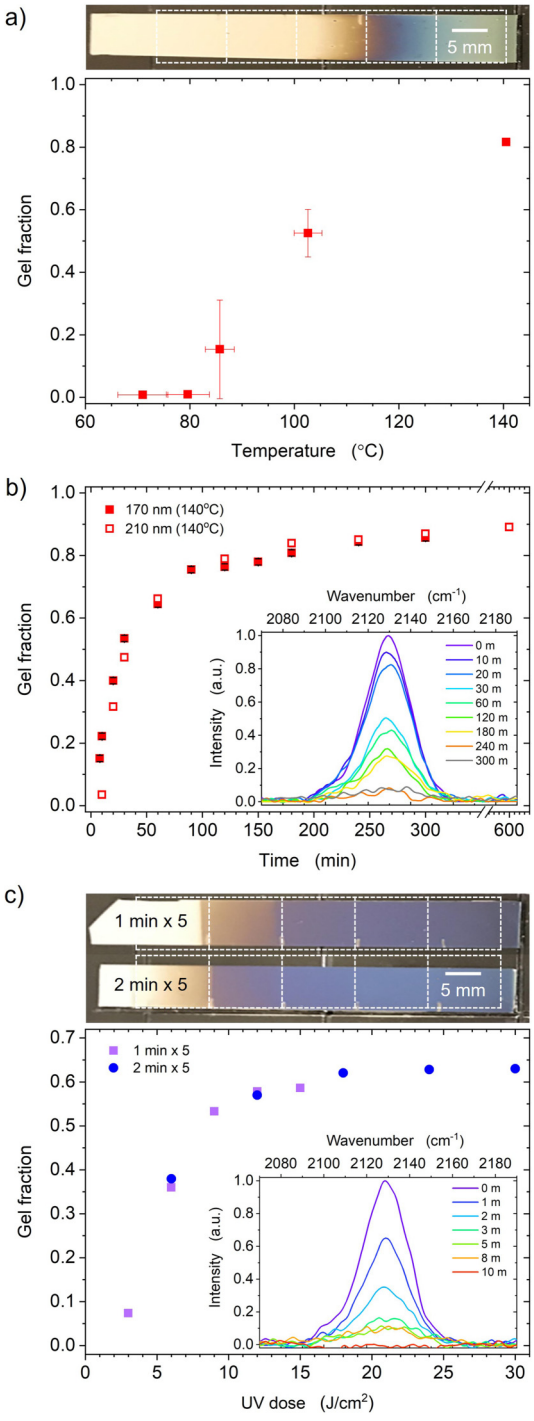

FIG. 2. Gel fraction of PVP/10% 4-ASPTMS as a function of (a) annealing temperature, (b) annealing time, and (c) UV dose. Inset figures in (b) and (c) are FTIR-ATR spectra of annealed and UV-irradiated samples, respectively. Color change in photographs denotes a change in the film thickness from which P_{gel} is determined. UV dose (J/cm^2) = UV incident power (W/cm^2) × time (s).

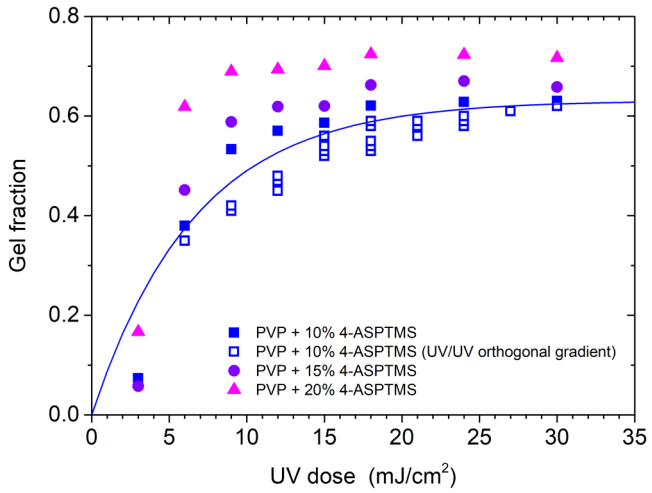

FIG. 3. Gel fraction of PVP/10% 4-ASPTMS, PVP/15% 4-ASPTMS, and PVP/20% 4-ASPTMS layers plotted against UV dose. All samples were irradiated at $\lambda = 254$ nm with a UV incident power = 50 mW/cm^2. Open square data from the PVP/10% 4-ASPTMS UV/UV orthogonal gradient sample. The line is the best fit to the PVP/10% 4-ASPTMS data: Gel fraction $= 0.631*[1 - \exp(-0.15*\text{UV dose})]$.

dose using a photomask and produced two uni-directional (discrete) gradients [cf. Fig. 2(c)]. In the first sample, the UV dose varies from 3 (first square from the left) to 15 J/cm^2 (fifth square from the left), and the second sample ranges from 6 (first square

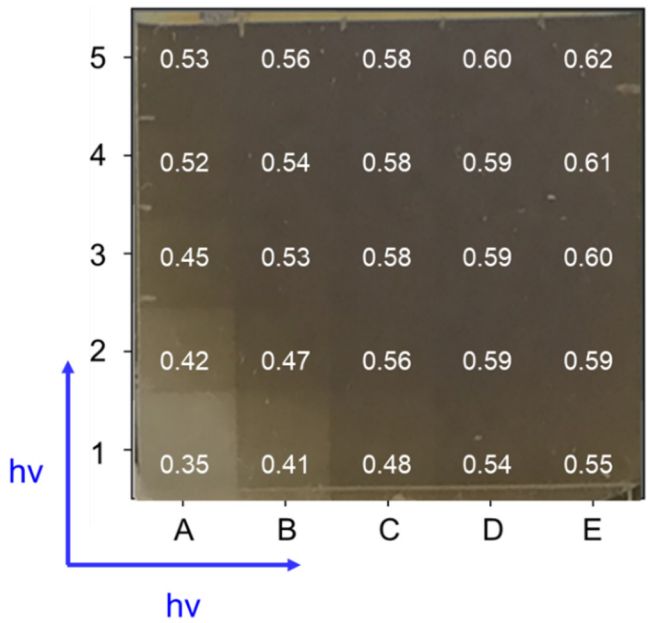

FIG. 4. Photograph of UV/UV discrete orthogonal gradient networks from PVP/10% 4-ASPTMS layers. Inset values denote the measured gel fraction at that square (1 × 1 cm^2). Sample size = 5 × 5 cm^2.

from the left) to 30 J/cm^2 (fifth square from the left). Figure 2(c) shows the measured P_{gel} against UV dose, where the maximum gelation ($P_{gel} = 0.60$) is attained after a dose of 15 J/cm^2 (5 min). The inset in Fig. 2(c) shows a gradual decrease in the absorbance of azide groups ($N = N^+=N^-$) at 2130 cm^{-1}. The signal nearly disappeared after 5 min, suggesting that almost all azide functionalities were consumed and formed sulfonamide links.

Our previous work established that PVP does not cross-link under UV light at 254 nm without 4-ASPTMS.[14] We studied the kinetics of UV-activated gel formation using PVP/4-ASPTMS mixtures with a variable content of 4-ASPTMS. As evidenced by the data in Fig. 3, increasing the content of 4-ASPTMS and the UV dose resulted in a higher P_{gel}. The gel-forming rate is faster for 20% (or 15%) than 10% 4-ASPTMS. As expected, the maximum P_{gel} is also higher for 20% (0.70) than 10% (0.60). These results are consistent with PVP/6-ASHTES and reveal that 4-ASPTMS concentration is another critical factor in gel formation.[11] In further studies, we use PVP/10% 4-ASPTMS as a model system.

Insights gained from thermally and UV-initiated PVP/10% 4-ASPTMS allowed us to identify the appropriate reaction conditions for generating orthogonal gradient networks. To begin with UV/UV orthogonal gradients, we prepared UV/UV discrete orthogonal gradients by depositing a thin layer (~170 nm) of PVP/10% 4-ASPTMS on a 5 × 5 cm^2 silicon wafer. Then, we used a photomask to control UV exposure time or UV dose by unmasking the sample by 1 cm/min in orthogonal directions. Figure 4 shows the original photograph of the sample exhibiting discrete orthogonal gradients in the film thickness from which the gel fraction is

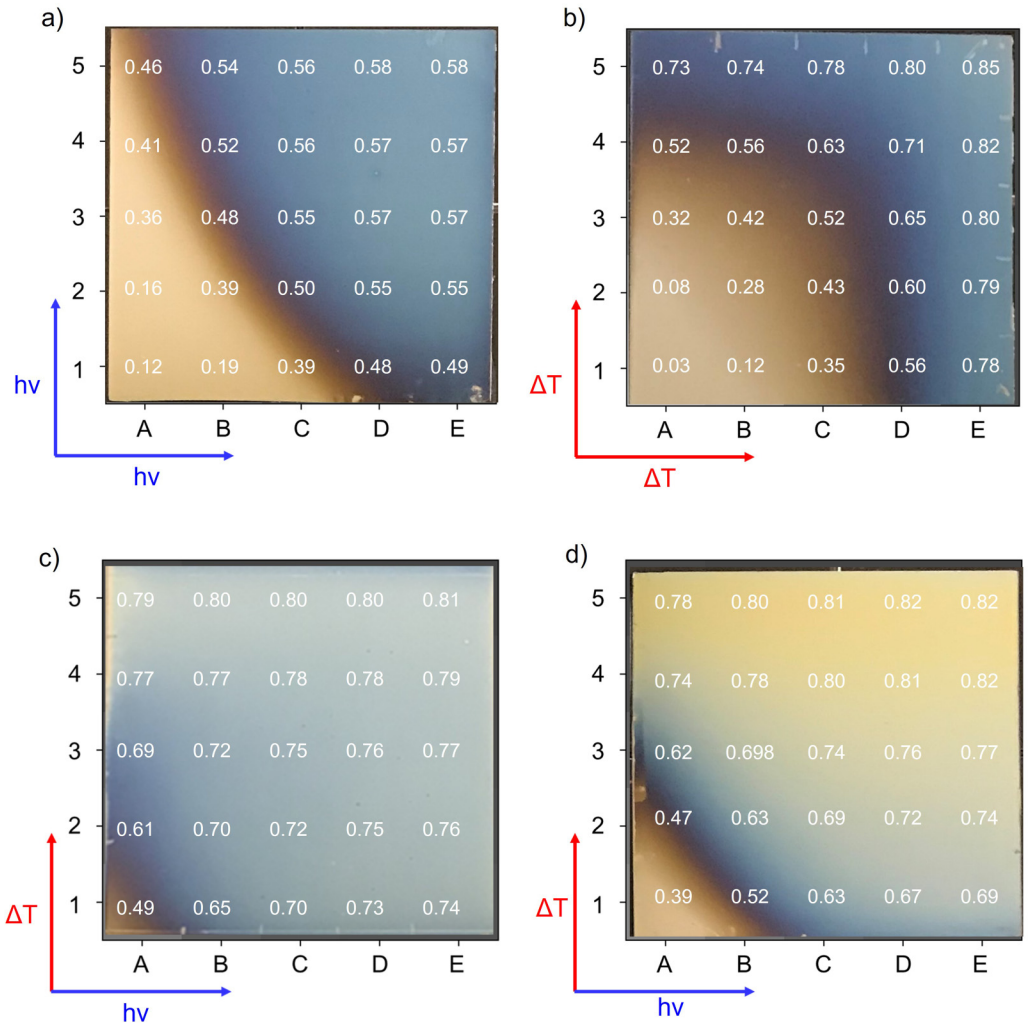

FIG. 5. Photographs of (a) UV/UV, (b) thermal/thermal, (c) UV/thermal, and (d) thermal/UV orthogonal gradient networks comprising PVP/10% 4-ASPTMS. The color change represents the variation in the film thickness from which the gel fraction (P_{gel}) is determined. Insert values denote the measured P_{gel} at that square (1 cm^2). Red and blue arrows symbolize the directions of gradients in temperature and UV dose, respectively. They increase from 1 → 5 or A → E. The overall sample size is 5 × 5 cm^2.

calculated using Eq. (1). The measured P_{gel} gradually increased from A → E or 1 → 5. For example, from A → E or 1 → 5, the exposure time increased gradually from 1 to 5 min. As a result, the total exposure time at A1 is 2 min (6 J/cm^2) and, for E5, is 10 min (30 J/cm^2). We plot the P_{gel} data from Fig. 4 in Fig. 3 against UV dose (as open squares) and find the consistent results (with minor deviations at low UV dose).

Concurrently, we synthesized a UV/UV continuous orthogonal gradient network, where the sample was moved under the UV lamp at the rate of 1 cm/min for 5 min. After the first run, the sample was rotated 90° clockwise and cross-linked for another 5 min at the same rate (1 cm/min). The sample was divided into a 5 × 5 matrix (i.e., 1 cm^2 × 25 squares), and the layer thickness was measured to determine P_{gel}. We measured 2–3 data points in each square (=1 cm^2) and plotted the average P_{gel} in Fig. 5(a). P_{gel} increased continuously from A → E or 1 → 5; i.e., A1 presents the lowest P_{gel} (~0.35), while E5 possesses the maximum P_{gel} (~0.58). The results are consistent with the discrete UV/UV orthogonal gradient sample in Fig. 4.

To investigate thermal/thermal orthogonal gradients, we deposited a thin layer (~170 nm) of PVP/10% 4-ASPTMS mixture on a silicon wafer with a dimension of 5 × 5 cm^2. The sample was placed on a hot gradient stage (from 70 to 140 °C) and annealed for 150 min. The sample was then rotated 90° (clockwise) and annealed for another 150 min. The temperature at different locations (i.e., A–E and 1–5) of the sample was monitored continuously using thermocouples attached to the hot stage. Figure 5(b) presents the photograph of orthogonal gradient networks after extraction, where the color change implies the change in the film thickness from which P_{gel} is determined (*vide infra*). The measured P_{gel} (inset values) increased progressively with increasing annealing temperature from A → E or 1 → 5, demonstrating gradients in P_{gel}, i.e., P_{gel} of A1 = 0.03, A5 = 0.73, and E1 = 0.78. Because the annealing temperature is varied orthogonally from A → E and 1 → 5, a continuous gradient is detected if we visualize the sample diagonally from A1 (annealed at 80 °C, P_{gel} = 0.03) → E5 (annealed at 140 °C, P_{gel} = 0.85).

We synthesized UV/thermal orthogonal gradient networks after establishing the UV/UV and thermal/thermal gradients. Specifically, we synthesized UV/thermal orthogonal gradient networks [cf. Fig. 5(c)]. A thin layer (190–240 nm) of PVP/10% 4-ASPTMS was deposited on a silicon wafer (5 × 5 cm^2). The sample was then UV cross-linked by moving it under UV light at the rate of 1 cm/min for 5 min. The sample was then rotated 90° clockwise and placed on a hot gradient stage where one end of the sample was maintained at 140 °C, and the other end was held at 75 °C (±5°). After cross-linking, the layers were extracted in methanol overnight and dried to measure the film thickness, from which we determined the gel fraction. Similarly, we generated thermal/UV orthogonal gradients where the sample was first annealed at 140 °C for 2.5 h on the hot gradient stage and then UV-cross-linked for 5 min (1 cm/min).

Figure 5(c) presents the original photograph of the UV/thermal gradient sample, where a color change denotes the change in the film thickness. Inset values depict the measured P_{gel} of the specimen featuring gradients in gel fraction prepared by UV cross-linking (A → E) followed by thermal cross-linking (1 → 5). P_{gel} increases from A1 → E1 or A1 → A5 and decreases from E5 → E1 or E5 → A5. Strongly cross-linked regions of the sample either thermally (A5, B5, C5, D5, and E5) or by UV-light (E1, E2, E3, E4, and E5) showed a high P_{gel} than the rest of the regions that reacted to a lesser degree by either of the cross-linking processes. The most significant P_{gel} increase is noted when examining the specimens diagonally from A1 → B2 → C3 → D4 → E5. Thus, the gel fraction change depends strongly on the extent to which the gel is reacted through UV or thermal cross-linking. Similar results were obtained for thermal/UV orthogonal gradients, where the sample was first cross-linked thermally and then UV cross-linked [cf. Fig. 5(d)].

IV. CONCLUSIONS AND OUTLOOK

We investigated the synthesis of surface-attached PVP gradient networks using a UV and thermally active 4-ASPTMS. Our results reveal that employing a single bi-functional gelator can effectively control the network's gel fraction by adjusting the UV and temperature in a gradient fashion. We successfully demonstrated the generation of orthogonal gradient networks, exhibiting gradients in gel fraction by regulating the UV dose and temperature in orthogonal directions. Furthermore, the gel fraction can be related to the degree of cross-linking, i.e., the higher the P_{gel}, the denser the network (strongly cross-linked), and similarly the lower the P_{gel}, the looser the network (soft).

We have recently measured the degree of swelling of surface-anchored PVP gels, α, i.e., the ratio of the thickness of the swollen gel and that of the dry gel, in water.[15] The gels were formed by thermally cross-linking PVP with 6-ASHTES. $\alpha = -15.254 * P_{gel} + 17.337$ in $P_{gel} \in (0.44, 0.98)$. We expect the gels formed by cross-linking PVP with 4-ASPTMS to follow the same trend.

Surface-anchored gels with a gradual variation in the gel density offer a convenient platform for high-throughput screening of protein adsorption. Loosely cross-linked gels swell in an aqueous medium and repel proteins due to entropic shielding and size-exclusion factors.[16–18] The gradient in hydrogel density will enable exploring protein adsorption systematically. Using 4-ASPTMS as a UV and thermally active cross-linker offers the ability to create complex gel fraction patterns on substrates. One may envision forming complex gel motifs featuring a continuous variation in P_{gel} via directional gradual thermal activation (large scale gradients, mm cm) with superimposed discrete local gel density patterns created by local UV activation (narrow scale gradients: μm cm).

ACKNOWLEDGMENTS

The work was supported by the S. Frank and Doris Culberson funds. Partial support under Grant No. DMR-1809453 is appreciated.

AUTHOR DECLARATIONS

Conflict of Interest

The authors have no conflicts to disclose.

Ethics Approval

Ethics approval is not required.

Author Contributions

C. K. Pandiyarajan: Conceptualization (supporting); Data curation (lead); Investigation (equal); Visualization (equal); Writing – original draft (lead); Writing – review & editing (equal). **Jan Genzer:** Conceptualization (lead); Project administration (lead); Supervision (lead).

DATA AVAILABILITY

The data that support the findings of this study are available within the article.

REFERENCES

[1]T. H. Kim, D. B. An, S. H. Oh, M. K. Kang, H. H. Song, and J. H. Lee, Biomaterials **40**, 51 (2015).
[2]J. Genzer, Annu. Rev. Mater. Res. **42**, 435 (2012).
[3]K. U. Claussen, T. Scheibel, H.-W. Schmidt, and R. Giesa, Macromol. Mater. Eng. **297**, 938 (2012).
[4]X. Dong, H. Zhao, J. Li, Y. Tian, H. Zeng, M. A. Ramos, T. S. Hu, and Q. Xu, iScience **23**, 101749 (2020).
[5]J. Genzer and R. R. Bhat, Langmuir **24**, 2294 (2008).
[6]B. R. Coad, K. E. Styan, and L. Meagher, ACS Appl. Mater. Interfaces **6**, 7782 (2014).
[7]D. Paripovic and H.-A. Klok, Macromol. Chem. Phys. **212**, 950 (2011).
[8]M. Brió Pérez, M. Cirelli, and S. de Beer, ACS Appl. Polym. Mater. **2**, 3039 (2020).
[9]S. K. Christensen, M. C. Chiappelli, and R. C. Hayward, Macromolecules **45**, 5237 (2012).
[10]C. K. Pandiyarajan, M. Rubinstein, and J. Genzer, Macromolecules **49**, 5076 (2016).
[11]C. K. Pandiyarajan and J. Genzer, Macromolecules **52**, 700 (2019).
[12]M. Körner, O. Prucker, and J. Rühe, Macromolecules **49**, 2438 (2016).
[13]K. Schuh, O. Prucker, and J. Rühe, Macromolecules **41**, 9284 (2008).
[14]C. K. Pandiyarajan and J. Genzer, Macromol. Rapid Commun. **42**, 2100266 (2021).
[15]S. Y. Woo, C. K. Pandiyarajan, and J. Genzer, ACS Appl. Polym. Mater. **3**, 5568 (2021).
[16]C. K. Pandiyarajan, O. Prucker, B. Zieger, and J. Rühe, Macromol. Biosci. **13**, 873 (2013).
[17]C. K. Pandiyarajan and J. Genzer, Langmuir **33**, 1974 (2017).
[18]O. Prucker, T. Brandstetter, and J. Rühe, Biointerphases **13**, 010801 (2018).